Fragmentation cross sections of Fe^{26+}, Si^{14+} and C^{6+} ions of 0.3 ÷ 10 A GeV on CR39, polyethylene and aluminum targets

M. Giorgini[a,b], for the BIOSHIELD-B44 and BINFRA-15B517 experiments*

[a]*Dept. of Physics, University of Bologna, I-40127 Bologna, Italy*
[b]*INFN-Bologna, I-40127 Bologna, Italy*

Talk given at the 24th International Conference on Nuclear Tracks in Solids, Bologna, Italy, 1-5 September 2008.

Abstract

New measurements of the total and partial fragmentation cross sections in the energy range 0.3 ÷ 10 A GeV of Fe^{26+}, Si^{14+} and C^{6+} beams on polyethylene, CR39 and aluminum targets are presented. The exposures were made at Brookhaven National Laboratory (BNL), USA, and Heavy Ion Medical Accelerator in Chiba (HIMAC), Japan. The CR39 nuclear track detectors were used to identify the incident and survived beams and their fragments. The total fragmentation cross sections for all targets are almost energy independent while they depend on the target mass. The measured partial fragmentation cross sections are also discussed.

1. Introduction

The interaction and propagation of intermediate and high energy heavy ions in matter is a subject of interest in the fields of astrophysics, radio-biology and radiation protection (Chen 1994).

Recently the attention was focused on nucleus-nucleus interactions at lab energies ≤10 AGeV, which are important for radiotherapy and radioprotection purposes. The FLUKA (Fassò 2003) MonteCarlo code was fused with the RQMD (Relativistic Quantum Molecular Dynamics) code (Garzelli 2006). It is important that the simulated data be continuously improved and confirmed by new experimental data, such as those presented here.

The availability of ion beams at the BNL (USA) and at the HIMAC (Japan) facilities made possible to investigate the projectile fragmentation on different targets and for different projectile energies.

The present study is focused on Fe^{26+}, Si^{14+} and C^{6+} ion interactions in CH_2, CR39 ($C_{12}H_{18}O_7)_n$ and Al targets. We used CR39 detectors, which are sensitive for a wide range of charges down to $Z = 6e$ in the low velocity and in the relativistic regions (Balestra 2007; Cecchini 1993; Cecchini 2001; Cecchini 2002; Dekhissi 2000; Giacomelli 1998). NTD's have been used to search for exotic particles like Magnetic Monopoles, Strange Quark Matter and Q-balls (Ambrosio 2002; Balestra 2008; Cecchini 2008; Medinaceli 2008; Sahnoun 2008), to study cosmic ray composition (Chiarusi 2005) and for environmental studies (Manzoor 2007).

*The **BIOSHIELD-B44** and **BINFRA-15B517** experiments: S. Cecchini, T. Chiarusi, G. Giacomelli, M. Giorgini, A. Kumar, G. Mandrioli, S. Manzoor, A.R. Margiotta, E. Medinaceli, L. Patrizii, V. Popa, I.E. Qureshi, Z. Sahnoun, G. Sirri, M. Spurio and V. Togo

2. Experimental procedure

Stacks composed of several CR39 NTD's, of size 11.5×11.5 cm^2, and of different targets were exposed to 0.3, 1, 3, 5 and 10 A GeV Fe^{26+}, 1, 3, 5 A GeV Si^{14+} ions at the BNL Alternating Gradient Synchrotron (AGS) and NASA Space Radiation Laboratory (NSRL). Our experiment, named BIOSHIELD-B44, was included in the time slots allocated to NASA for a program of space radiation research. For these low dose experiments, an ionization chamber was used as monitor. It was calibrated with a 1×1 mm^2 scintillation counter placed at the center of the beam. The beam density was monitored with a pixel counter (Lowenstein, D.I. and Rusek, A., 2007) and later checked with our nuclear track detectors.

The exposures to 0.41 A GeV Fe^{26+}, 0.29 A GeV C^{6+} ions at HIMAC were performed in collaboration with colleagues from Naples and Japan. The experiment was named BINFRA-15B517. In this case, the beam was monitored with a photographic sheet, as explained in details in Durante 2002.

For our fragmentation studies, we used three and four CR39 sheets, ∼0.7 mm thick, placed before and after the target, respectively. The exposures were done at normal incidence, with a density of ∼2000 ions/cm^2.

After exposures the CR39 foils were etched in 6N NaOH aqueous solution at 70 °C for 30 h (in two steps 15h+15h) in a thermostatic water bath with constant stirring of the solution. After etching, the beam ions and their fragments manifest in the CR39 NTD's as etch pit cones on both sides of each detector foil.

The total charge changing cross sections were determined from the survival fraction of ions using the following relation

$$\sigma_{tot} = \frac{A_T \ln(N_{in}/N_{out})}{\rho \, t \, N_{Av}} \quad (1)$$

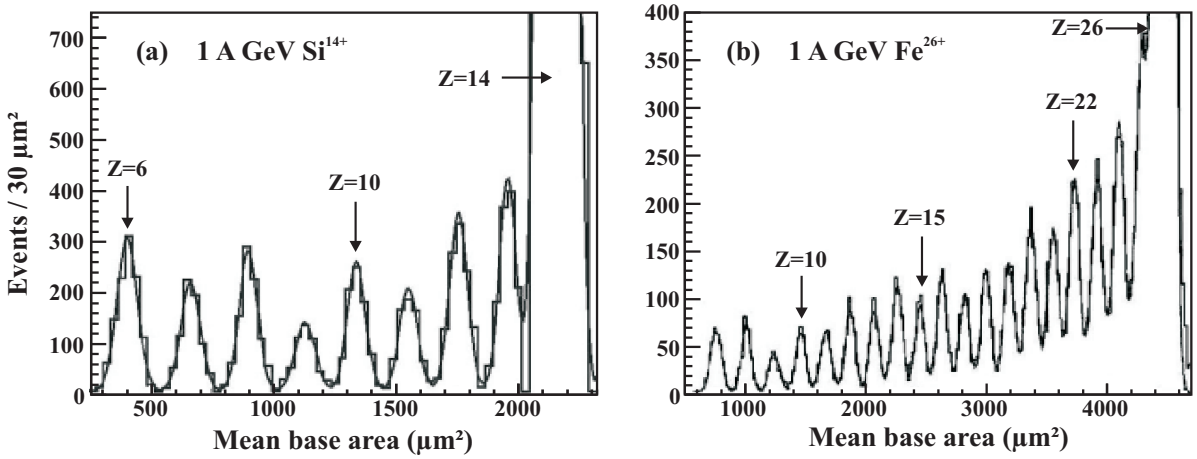

Figure 1: Distributions of the average base areas for tracks present in at least 2 out of 3 measured CR39 sheets located after the CH_2 target. The data concern (a) 1 A GeV Si^{14+} and (b) 1 A GeV Fe^{26+} ions. Each peak has a gaussian shape with $\sigma \sim 0.2e$.

where A_T is the nuclear mass of the target (average nuclear mass in case of polymers: $A_{CH2} = 4.7$, $A_{CR39} = 7.4$); N_{in} and N_{out} are the numbers of incident ions before and after the target, respectively; ρ (g/cm^3) is the target density; t (cm) is the thickness of the target and N_{Av} is Avogadro number.

Systematic uncertainties in σ_{tot} were estimated to be smaller than 10%: contributions arise from the measurements of the density and thickness of the targets, from the separation of the beam peak from the fragments immediately close by (Fig. 1), from fragmentation in the CR39 foils and from the tracking procedure.

The base areas of the etch-pit cones ("tracks"), their eccentricity and central brightness were measured with an automatic image analyzer system (Noll 1988) which also provides their absolute coordinates. A tracking procedure was used to reconstruct the path of beam ions through the front faces of the detector upstream (with respect to the target) foils; a similar tracking procedure was performed through the three measured front faces of downstream CR39 detectors. The average track base area was computed for each reconstructed ion path by requiring the existence of signals in at least two out of three sheets of the detectors. In Fig. 1a,b the average base area distributions for 1 A GeV Si^{14+} and 1 A GeV Fe^{26+} beam ions and their fragments after the CH_2 targets are shown.

3. Total fragmentation cross sections

The numbers of incident and survived beam ions were determined considering the mean area distributions of the beam peaks before and after the target and evaluating the integral of the gaussian fit of the beam peaks.

The measured total charge changing cross sections are given in the 4th column of Table 1. Fig. 2a shows the total cross sections of Fe^{26+} projectiles at various beam energies on the CH_2 and Al targets. Our results for Si^{14+} and C^{6+} projectiles are given in Table 2 and are plotted vs energy in Fig. 2b.

Energy (A GeV)	Target	A_T	σ_{tot} (mb)
10	CH_2	4.7	1147 ± 97
10	CR39	7.4	1105 ± 360
5	CH_2	4.7	1041 ± 130
5	CR39	7.4	1170 ± 470
3	CH_2	4.7	904 ± 140
3	CR39	7.4	1166 ± 67
1	CH_2	4.7	1105 ± 60
1	CR39	7.4	1113 ± 176
1	Al	27	1870 ± 131
0.41	CH_2	4.7	948 ± 54
0.41	CR39	7.4	1285 ± 245
0.41	Al	27	1950 ± 126
0.30	CH_2	4.7	949 ± 61
0.30	CR39	7.4	1174 ± 192
0.30	Al	27	2008 ± 144

Table 1: Total fragmentation cross sections, with statistical standard deviations, for Fe^{26+} ions of different energies (col. 1) on different targets (col. 2).

The total cross sections are almost energy independent, in agreement with the data from other authors (Brechtmann 1988; Brechtmann 1989; Flesch 2001; Zeitlin 1997; Zeitlin 2007).

In Fig. 2 our data are compared with the semi-empirical formula (Bradt, H.L. and Peters, B., 1950) for nuclear cross sections (solid lines)

$$\sigma_{tot} = \pi r_0^2 \, (A_P^{1/3} + A_T^{1/3} - b_0)^2 \qquad (2)$$

where $r_0 = 1.31$ fm, $b_0 = 1.0$, A_P and A_T are the projectile and target mass numbers, respectively.

Figs. 3a,b show the total fragmentation cross sections vs target mass number A_T for Fe^{26+}, Si^{14+} and C^{6+} beams of various energies. The solid lines are the predictions of Eq. 2, to which we added the electromagnetic dissociation contribution,

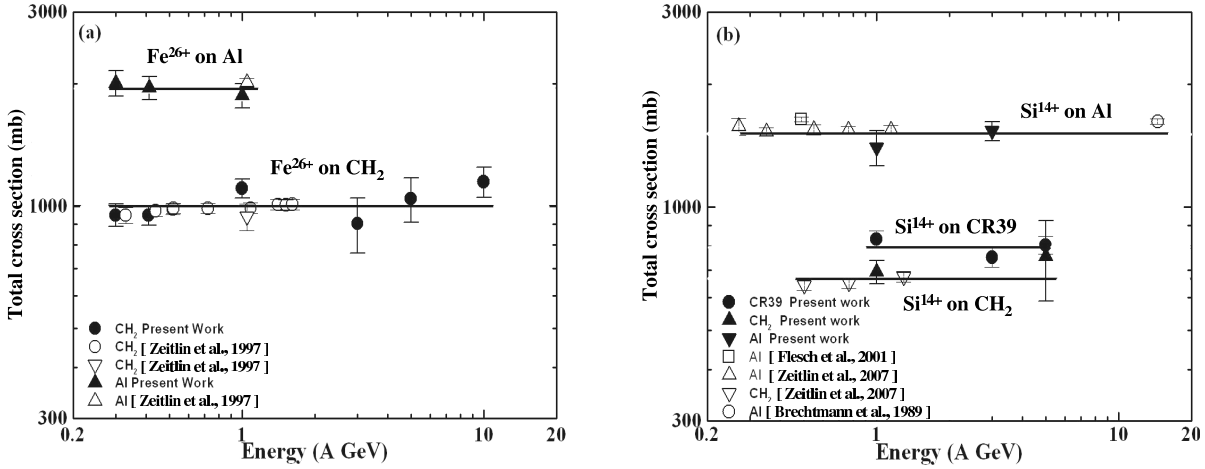

Figure 2: Total fragmentation cross sections for (a) Fe^{26+} ions of different energies in CH_2 and Al targets and (b) for Si^{14+} ions in CH_2, CR39 and Al targets. The measured cross sections from the cited refs. and the predictions from Eq. 2 are shown for comparison.

Si^{14+} ions			C^{6+} ions		
Energy (A GeV)	**Target**	σ_{tot} **(mb)**	**Energy (A GeV)**	**Target**	σ_{tot} **(mb)**
5	CH_2	757 ± 168	0.29	CH_2	460 ± 53
3	Al	1533 ± 133	0.29	CR39	513 ± 52
1	CR39	1113 ± 176	0.29	Al	1155 ± 108
1	H	483 ± 76			
1	CH_2	694 ± 70			
1	C	1117 ± 62			
1	Al	1397 ± 138			

Table 2: Total fragmentation cross sections, with statistical standard deviations, for Si^{14+} ions of different energies (col.1) on different targets (col. 2) and for 0.29 A GeV C^{6+} ions on different targets (col. 5).

$\sigma_{EMD} = \alpha Z_T^{\delta}$, with $\alpha = 1.57$ fm^2 and $\delta = 1.9$ (Dekhissi 2000). The total fragmentation cross sections increase with increasing target mass number. Part of the increase is due to the effect of electromagnetic dissociation.

The data from other authors (Brechtmann 1988; Brechtmann 1989; Golovchenko 1999; Golovchenko 2002; Zeitlin 1997; Zeitlin 2007) are plotted for comparison and show good agreement with our data, within the experimental uncertainties.

4. Partial fragmentation charge changing cross sections

If the thickness of the target is small compared to the mean free path of the fragments in that material, the partial fragmentation cross sections can be calculated using the simple relation

$$\sigma(Z_i, Z_f) \simeq \frac{1}{Kt}\frac{N_f}{N_i} \tag{3}$$

where $\sigma(Z_i, Z_f)$ is the partial fragmentation cross section of an ion Z_i into the fragment Z_f, K is the number of target nuclei per cm^3, t is the thickness of the target, N_i is the number of survived ions after the target and N_f is the number of fragments produced with charge Z_f. This expression may be valid also for a thick target, assuming that the number of fragments before the target is zero.

For the Fe^{26+} ions, we observed that fragments are present even before the targets. In this case the partial charge change cross sections have been computed via the relation

$$\sigma_{\Delta Z} = \frac{1}{Kt}\left(\frac{N_{out}^f}{N_s^p} - \frac{N_{in}^f}{N_{in}^p}\right) \tag{4}$$

where N_{in}^f and N_{out}^f are the numbers of fragments of each charge before and after the target, and N_{in}^p and N_s^p are the numbers of incident and survived projectile ions.

The distributions, after the CH_2 targets, of the fragments for 1 A GeV Si^{14+} and 1 A GeV Fe^{26+} ions are shown in Figs. 1a,b. The relative partial fragmentation cross sections for $\Delta Z = -1, -2, -3, .., -18$ are given in Table 3. The quoted errors are statistical standard deviations; systematic uncertainties are estimated to be about 10%. A clear odd-even effect is visible in Fig. 1: the cross sections for the $Z-$even fragments are generally larger than those for the $Z-$odd fragments close by.

5. Conclusions

The total fragmentation cross sections for Fe^{26+}, Si^{14+} and C^{6+} ion beams of $0.3 \div 10$ A GeV energies on polyethylene, CR39 and aluminum targets were measured using CR39 NTD's.

The total cross sections for all the targets and energies used in the present work do not show any observable energy dependence. There is a dependence on target mass; the highest cross sections are observed for Al targets and this is mainly due to the contribution of electromagnetic dissociation. The present data of total fragmentation cross sections are in agreement with similar experimental data in the literature (Brechtmann 1988;

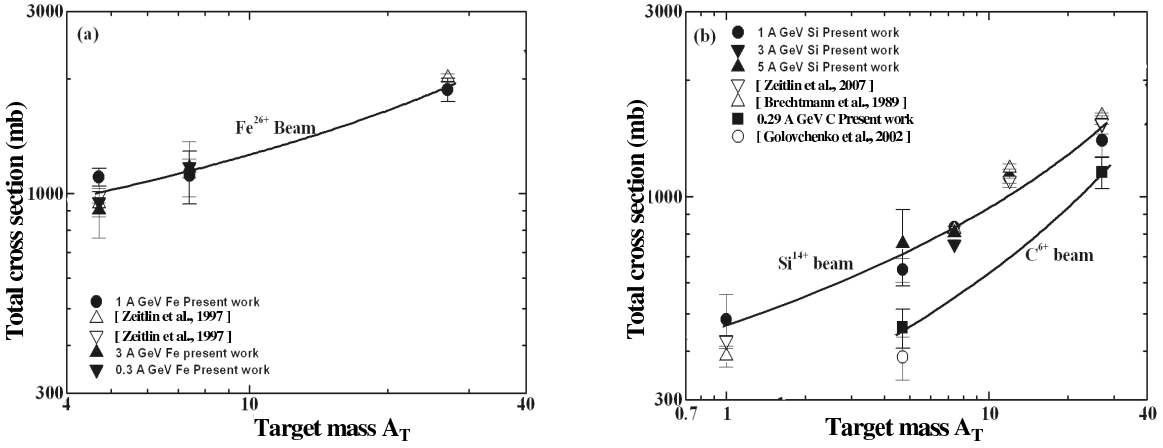

Figure 3: Total fragmentation cross sections vs the target mass (a) for Fe^{26+} ions and (b) for Si^{14+} and C^{6+} ions. The measured cross sections from the cited refs. are shown for comparison. The solid lines are from Eq. 2 corrected by the σ_{EMD} term.

ΔZ	1 A GeV Fe^{26+}	1 A GeV Si^{14+}
-1	-	293 ± 18
-2	338 ± 11	177 ± 12
-3	285 ± 11	123 ± 11
-4	252 ± 10	122 ± 11
-5	249 ± 10	62 ± 8
-6	197 ± 9	117 ± 11
-7	168 ± 8	83 ± 9
-8	132 ± 7	90 ± 10
-9	175 ± 8	
-10	107 ± 7	
-11	152 ± 6	
-12	105 ± 8	
-13	103 ± 6	
-14	81 ± 6	
-15	80 ± 6	
-16	50 ± 4	
-17	76 ± 5	
-18	86 ± 6	

Table 3: Partial fragmentation charge changing cross sections, with statistical standard deviations, for 1 AGeV Si^{14+} and Fe^{26+} ions on the CH_2 targets.

Brechtmann 1989; Cecchini 2002; Dekhissi 2000; Flesch 2001; Golovchenko 1999; Golovchenko 2002; Zeitlin 1997; Zeitlin 2007).

The presence of well separated fragment peaks, see Fig. 1, allowed the determination of the partial fragmentation cross sections. On the average the partial cross sections decrease as the charge change ΔZ increases. The data in Fig. 1 and the partial cross sections in Table 3 indicate a clear Z odd-even effect.

The measured cross section data indicate that passive NTD's, specifically CR39, can be used effectively for studies of the total and partial charge changing cross sections, also in comparison with active detectors.

Acknowledgments

We acknowledge the grants NRA-02-OBPR-02 and 15B517 for the BIOSHIELD and BINFRA experiments, respectively.

We thank the technical staff of BNL and HIMAC for their kind cooperation during the beam exposures and the contribution of our technical staff. We thank INFN and ICTP for providing fellowships and grants to non-Italian citizens.

References

Ambrosio, M. et al., 2002. Eur. Phys. J. C25, 511.
Balestra, S. et al., 2007. Nucl. Instr. Meth. B254, 254.
Balestra, S. et al., 2008. Eur. Phys. J. C55, 57.
Bradt, H.L. and Peters, B., 1950. Phys. Rev. 77, 54.
Brechtmann, C. et al., 1988. Z. Phys. A330, 407.
Brechtmann, C. et al., 1989. Phys. Rev. C39, 2222.
Cecchini, S. et al., 1993. Astrop. Phys. 1, 369.
Cecchini, S. et al., 2001. Radiat. Meas. 34, 55.
Cecchini, S. et al., 2002. Nucl. Phys. A707, 513.
Cecchini, S. et al., 2008. arXiv:0805.1797 [hep-ex].
Chen, C.X. et al., 1994. Phys. Rev. C49, 3200.
Chiarusi, T. et al., 2005. Radiat. Meas. 40, 424.
Dekhissi, H. et al., 2000. Nucl. Phys. A662, 207.
Durante, M. et al., 2002. J. Radiat. Res. 43, S107.
Fassò, A. et al., 2003. arXiv:hep-ph/0306267.
Flesch, F. et al., 2001. Radiat. Meas. 34, 237.
Garzelli M.V. et al., 2006. J. of Phys. Conf. Series 41, 519.
Giacomelli, G. et al., 1998. Nucl. Instr. Meth. A411, 41.
Golovchenko, A.N. et al., 1999. Nucl. Instr. Meth. B159, 233
Golovchenko, A.N. et al., 2002. Phys. Rev. C66, 014609.
Lowenstein, D.I. and Rusek, A., 2007. Radiat. Environ. Biophys. 46, 91.
Manzoor, S. et al., 2007. Nucl. Phys. B Proc. Suppl. 172, 92.
Medinaceli, E. et al., 2008. These Proceedings.
Noll, A. et al., 1988. Nucl. Tracks Radiat. Meas. 15, 265.
Sahnoun, Z. et al., 2008. These Proceedings.
Zeitlin, C. et al., 1997. Phys. Rev. C56, 388.
Zeitlin, C. et al., 2007. Nucl. Phys. A784, 341.